

New photocleavable structures III: Photochemistry and photophysics of pyridinoyl and benzoyl-based photoinitiators

Bernhard Seidl^a, Robert Liska^{a,*}, Gottfried Grabner^b

^a Institute of Applied Synthetic Chemistry, Division Macromolecular Chemistry, University of Technology, Getreidemarkt 9/163MC, 1060 Vienna, Austria

^b Max F. Perutz Laboratories, Institute of Biomolecular Structural Biology, University of Vienna, Campus-Vienna-Biocenter 5, 1030 Vienna, Austria

Received 1 July 2005; received in revised form 6 September 2005; accepted 30 September 2005
Available online 18 November 2005

Abstract

Pyridine ketones have recently been found to be suitable α -cleavage photoinitiators for radical polymerization with excellent water solubility. Nanosecond time-resolved laser flash photolysis and steady-state photolysis were employed to study and compare the triplet photophysics and the photochemistry of 2-hydroxy-2-methyl-1-pyridin-3-yl-propan-1-one (**1b**) and its commercial benzoyl analogue 2-hydroxy-2-methyl-1-phenylpropan-1-one (Darocur 1173[®], **1a**), and of some of their less photoreactive derivatives, in acetonitrile solution. The triplet state quantum yield, measured by energy transfer to naphthalene, was smaller for **1b** ($\Phi_T = 0.10$) than for **1a** ($\Phi_T = 0.25$), but the photodegradation quantum yields in the presence of the radical trap TEMPO were comparable ($\Phi_D = 0.6$). The discrepancy between the yields of triplet formation and photodegradation points to a possible role of higher excited triplet states in the process of photoinduced α -cleavage. The reactivities of the primary radicals with a series of reaction partners showed that the benzoyl and the nicotinoyl radical have comparable reactivities towards polymerizable double bonds, but that the nicotinoyl radicals reacts 17 times faster with TEMPO. The previously observed reduced oxygen sensitivity in photopolymerization using **1b** compared to **1a** could be traced to a smaller reactivity towards O₂ of the nicotinoyl radical compared to the benzoyl radical. The photodegradation kinetics of **1a** and **1b** under steady-state conditions were comparable, but significant differences were observed in a photoproduct study.

© 2005 Elsevier B.V. All rights reserved.

Keywords: Photoinitiator; Time-resolved laser flash photolysis; α -Cleavage; Pyridine ketone

1. Introduction

Radiation curing is a well established and highly efficient method for crosslinking of coatings, printing inks, etc. [1]. Photoinitiators [2], the key component in such systems have a great influence on storage life, curing rate and curing depth, but also on double bond conversion (DBC) and surface cure. Among the large group of known photoinitiator structures, hydroxyalkylphenones, such as 2-hydroxy-2-methyl-1-phenylpropan-1-one (**1a**) (Darocur 1173) (Fig. 1) have gained much interest due to their high reactivity and universal applicability. A possible strategy to further improve the efficiency of these photoinitia-

tors is to modify them chemically in the position para to the benzoyl chromophore. Substitution by thioethers and especially by dialkylamino groups has been found to strongly influence the performance of hydroxyalkylphenones by changing photophysical properties, such as UV absorption, triplet energy, and triplet lifetime [3]. Modification of the hydroxy group by ethers does not change the photochemistry and reactivity, but acetyl derivatives in this position result in the loss of photoreactivity [3].

In this line of research, the contribution of our group has been focused during the last years on alternatives to the phenyl moiety. Hydroxyalkylphenone-analogous structures based on electron-rich heterocycles [4], such as furan, thiophene and pyrrole exhibited only poor photoinitiating activities [5]. From other heteroaromatic ketones like acetylthiophene and acetylfuran it is known that their lowest triplet state has π - π^* character [6], and therefore cannot lead to α -cleavage. In contrast, electron-

* Corresponding author. Tel.: +43 1 58801 16273; fax: +43 1 58801 16299.
E-mail addresses: seidl@otech7.tuwien.ac.at (B. Seidl),
robert.liska@tuwien.ac.at (R. Liska), gottfried.grabner@univie.ac.at (G. Grabner).

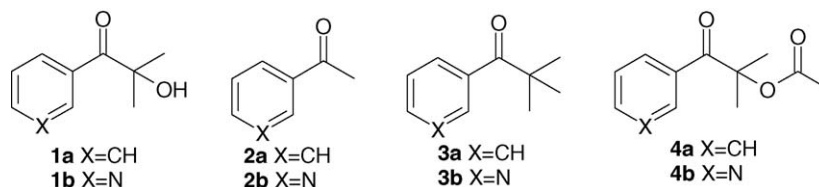


Fig. 1. Reference and pyridine based initiators.

poor heterocycles, such as pyridine were found to be highly reactive [7]. Investigations of the influence of the position of substituents on the pyridine ring showed highest activity for the 3-substituted derivative 2-hydroxy-2-methyl-1-pyridin-3-ylpropan-1-one (**1b**). Steady-state photolysis experiments and product analysis have proven that the α -cleavage process is the main photochemical pathway; this result, along with those of photo-DSC measurements, indicated that the photoinitiating behavior of **1b** is comparable to that of the commercially available initiator **1a** [7]. Characteristic differences in the photochemistry of both compounds were nevertheless suggested by these investigations; in particular, photo-DSC measurements in presence of air showed that **1b** is less susceptible to oxygen inhibition than **1a**. Furthermore **1b** has shown excellent water solubility (4.9 g/100 g) [7] and the applicability in water borne formulations is currently under investigation.

The photophysics and photochemistry of 3-pyridine ketones has been occasionally studied in the past. The triplet state of 3-acetylpyridine (**2b**) has been investigated by phosphorescence spectroscopy [8]. The photoreduction of **2b** in isopropanol was studied by Traynard and Blanchi [9]. Wagner showed type II photoelimination of 1-pyridin-3-yl-pentan-1-one in benzene [10,11]. The candidate photoinitiator **1b** and its derivatives **3b** and **4b** have not been studied previously.

It was therefore of interest to investigate the triplet photophysics and mechanistic photochemistry of initiator **1b** by means of laser flash photolysis experiments. Because the known fast photocleavage of **1a** (triplet lifetime, $\tau_T < 1$ ns) [3] suggested a similar behavior of **1b**, we decided to study and compare several analogous phenyl ketones and pyridine ketones with varying photochemical properties (Fig. 1). Similar photophysics were expected for acetophenone **2a** and acetylpyridine **2b** as the simplest ketones. Pivalophenone (**3a**) was known to exhibit significantly longer lived triplet states [12] compared to hydroxyalkylphenone **1a**; the analogous compound in our series is 2,2-dimethyl-1-pyridin-3-ylpropan-1-one (**3b**). Finally, the acetic acid 1,1-dimethyl-2-oxo-2-phenylethyl ester (**4a**) is non-cleavable [3] and so should be the acetic acid 1,1-dimethyl-2-oxo-2-pyridin-3-ylethyl ester (**4b**).

The photochemical efficiencies of **1a** and **1b** were additionally compared under steady-state photolysis conditions, using TEMPO as an efficient radical quencher to determine the rates and quantum yields of decomposition. Finally, laser flash photolysis experiments were carried out to study the comparative reactivities of the radicals produced upon photocleavage of **1a** and **1b** with several reaction partners (molecular oxygen, TEMPO and methyl methacrylate).

2. Experimental

2.1. Materials

All reagents were purchased from Sigma–Aldrich and used without further purification. The reference photoinitiator **1a** (Darocur 1173[®]) was received from Ciba SC as a gift and distilled under vacuum before use (bp: 84 °C/4 mm Hg). All reactions were carried out under inert atmosphere using solvents dried and purified by standard laboratory methods. Thin-layer chromatography was carried out with Alugram Sil-G/UV 254 sheets (Macherey Nagel). Column chromatography was performed on Merck silica gel 60 (0.063–0.200 mm).

2.2. Characterization

¹³C NMR and ¹H NMR spectra were recorded on a Bruker AC-E-200 FT-NMR-spectrometer; deuterated chloroform (CDCl₃) was used as solvent. GC/MS was performed on a Hewlett Packard 5890/5970 B system (Quadrupole) with a fused silica capillary column SPB-5 (60 m × 0.25 mm). UV spectra were recorded on a Hitachi U-2001 spectrophotometer. A reversed-phase HP-1100 HPLC system with DAD-detector was used for quantitative analysis of photodecomposition products. All separations were carried out on a XTerra MS C₁₈ column, particle size: 5 μ m, 150 mm × 3.9 mm i.d. (Waters). A linear gradient, with flow 0.8 ml/min, was formed from 100% water to 100% acetonitrile over a period of 30 min.

2.3. Syntheses

The following substances were prepared using published procedures: 3,3'-pyridil [13]; **1b** [7] (without isolating the THP-protected form; mp: 42–44 °C); pivaloyl ketone **3b** [14]; benzoic acid 2-oxo-1,2-diphenyl-ethyl ester [15] and 2-methyl-1-phenyl-1,2-propanediol [16].

2.3.1. Acetic acid 1,1-dimethyl-2-oxo-2-pyridin-3-yl-ethyl ester (**4b**)

4b was prepared by refluxing 0.79 g (4.8 mmol) of **1b** with 4.90 g (48 mmol) of acetic anhydride in 20 ml of dry acetonitrile for 48 h under a nitrogen atmosphere. After removal of the solvent under vacuum, the residue was dissolved in ether (20 ml), extracted with saturated aqueous NaHCO₃ (3 × 10 ml) and water (10 ml). The organic layer was dried with NaSO₄ and the solvent was removed under reduced pressure. The crude product was purified by column chromatography (petroleum ether/ethyl acetate, 1:2) to give 0.5 g (51%) of the title compound as pale yellow solid. mp: 67–69 °C.

^1H NMR (CDCl_3): δ (ppm) = 9.22 (s, 1H, ar-H); 8.70 (d, 1H, ar-H); 8.26 (d, 1H, ar-H); 7.37 (dd, 1H, ar-H); 1.94 (s, 3H, CH_3); 1.26 (s, 6H, CH_3); ^{13}C NMR (CDCl_3): δ (ppm) = 197.84 (ar-CO); 170.24 (COOCH_3); 152.58 (ar- C^6); 149.06 (ar- C^2); 136.18 (ar- C^4); 130.21 (ar- C^3); 123.65 (ar- C^5); 83.98 (C_q); 24.76 ($2 \times \text{CH}_3\text{-C}$); 21.19 ($\text{CH}_3\text{-CO}$); GC-MS: (m/z) = 207 (M^+), 179, 149, 121, 106, 79, 59, 51, 43; calc. for $\text{C}_{11}\text{H}_{13}\text{NO}_3$: C 63.76, H 6.32, N 6.76; found: C 63.88, H 6.41, N 6.59.

2.3.2. Benzoic acid 2,2,6,6-tetramethyl-piperidin-1-yl ester (**5a**) and nicotinic acid 2,2,6,6-tetramethyl-piperidin-1-yl ester (**5b**)

A solution of the initiators **1a** (2.00 g; 12 mmol) or **1b** (2.00 g; 12 mmol) and TEMPO (6.13 g; 36 mmol) in 400 ml dry acetonitrile was filled into a photoreactor, purged with argon for 10 min and irradiated with a high-pressure mercury lamp for 2 h. After full conversion of the initiator (monitored by TLC or GC-MS) the solvent was removed under reduced pressure and TEMPO was removed by kugelrohr distillation (65 °C/4 mm). The crude product was recrystallized from ethanol/water, 1:1.

5a was obtained in 63% yield as white crystals. mp: 90–92 °C.

^1H NMR (CDCl_3): δ (ppm) = 8.08 (d, 2H, ar-H), 7.61–7.42 (m, 3H, ar-H), 1.79–1.44 (m, 6H, $3 \times \text{CH}_2$), 1.27 (s, 6H, $2 \times \text{CH}_3$), 1.12 (s, 6H, $2 \times \text{CH}_3$); ^{13}C NMR (CDCl_3): δ (ppm) = 166.09 (Ar-COO-), 132.60 (ar- C^4), 129.29 (ar- C^2 , ar- C^6), 129.50 (ar- C^1), 128.20 (ar- C^3 , ar- C^5), 60.13 ($2 \times \text{C}_q\text{-}(\text{CH}_3)_2$), 38.83 ($2 \times \text{-C}_q\text{-CH}_2\text{-CH}_2\text{-}$), 31.73 ($2 \times \text{-CH}_3$), 20.61 ($2 \times \text{-CH}_3$), 16.77 ($\text{-CH}_2\text{-}$); GC-MS: (m/z) = 261 (M^+), 246, 156, 122, 105, 83, 77, 69, 55.

5b was obtained in 75% yield as white crystals. mp: 87–90 °C.

^1H NMR (CDCl_3): δ (ppm) = 9.30 (d, 1H, ar- H_2), 8.83 (d, 1H, ar- H_6), 8.38 (m, 1H, ar- H_4), 7.45 (m, 1H, ar- H_5), 1.50–1.80 (m, 6H, $3 \times \text{CH}_2$), 1.59 (s, 6H, $2 \times \text{CH}_3$), 1.33 (s, 6H, $2 \times \text{CH}_3$); ^{13}C NMR (CDCl_3): δ (ppm) = 165.1 (C=O), 153.5 (ar- C^6), 150.5 (ar- C^2), 137.3 (ar- C^4), 125.6 (ar- C^3), 123.6 (ar- C^5), 60.5 ($\text{C}_q\text{-N}$), 39.8 (CH_2), 31.9 (CH_3), 20.8 (CH_3), 16.9 (CH_2); GC-MS: (m/z) = 262 (M^+), 247, 156, 138, 123, 106, 78, 69, 55, 39; calc. for $\text{C}_{15}\text{H}_{22}\text{N}_2\text{O}_2$: C, 68.67; H, 8.45; N, 10.68; found: C, 68.37; H, 8.68; N, 10.35.

2.4. Time-resolved UV-vis spectroscopy

Triplet states and radicals were studied by transient absorption spectroscopy in a setup described earlier [17]. Sample solutions with concentrations of 5×10^{-4} to 1×10^{-3} M (266 nm) or 1×10^{-2} to 2×10^{-2} M (355 nm) in spectrophotometric grade acetonitrile were irradiated in rectangular quartz cells with 10 ns light flashes ($\lambda = 355$ or 266 nm) from a Nd:YAG-laser (Quanta-Ray DCR-1). Except for the measurements with oxygen the samples were purged with argon before and during irradiation. The pulse energy could be varied from 0.25 to 10 mJ/pulse.

2.5. Steady-state photolysis

Preparative photolysis experiments were carried out in a Heraeus UV reactor system UV-RS-1 (400 ml) equipped with a 150 W medium-pressure mercury lamp (TQ-150).

Photolysis experiments for kinetic investigations were carried out in a glass tube ($l = 15$ cm, i.d. = 1.5 cm) with ground joints at both endings and two adaptors with teflon septa on the side-walls. [18] A self-made quick-fit (cone/screw thread adaptor) closed on one end with a quartz window was connected to one ground joint. A light guide using a Efos Novacure (instrument setting 1500 mW/cm²) as irradiation source was attached to the window and the samples were magnetically stirred and irradiated with filtered UV light (365 nm). The solution was purged with argon before and during irradiation.

The *o*-nitrobenzaldehyde actinometer [19] was used to determine the total absorbed light intensity to be 1.61×10^{-5} Einstein $l^{-1} s^{-1}$. Quantitative analysis was carried out by HPLC with samples taken after 0, 1, 2, 5, 10, 20 and 30 min.

3. Results and discussion

3.1. Triplet photophysics

For direct measurement of the triplet-triplet absorption of the hydroxyalkylphenones **1a** the time resolution of our laser flash photolysis setup was insufficient. Because similar fast photochemistry was expected for **1b**, the triplet spectra of the other pyridine ketones were studied first.

Upon irradiation at 266 nm in acetonitrile (MeCN), the compounds **2b**, **3b** and **4b** afforded readily detectable triplet-triplet absorption spectra; the assignment was based on quenching by molecular oxygen and energy transfer to naphthalene or anthracene. For all three ketones, the spectra exhibited broad bands with maxima in the 410–430 nm region and the onset of a more intense band at $\lambda < 360$ nm, the latter being less pronounced for **4b** (Fig. 2). For comparison, **2a** has been described to give two maxima at 406 and 449 nm in cyclohexane [20]. **3a** in benzene has shown three bands at 335, 400 and 450 nm [12] and **4a** exhibited a triplet-triplet absorption maximum at 335 nm in MeCN [3].

The triplet lifetimes obtained in argon-purged solutions were $\tau_{T2b} = 3.0 \mu\text{s}$, $\tau_{T3b} = 0.17 \mu\text{s}$, and $\tau_{T4b} = 1.5 \mu\text{s}$. Short τ_T in absence of a quencher like oxygen indicates a fast and efficient intramolecular photochemistry (α -cleavage, H-abstraction) of these compounds. Twice longer τ_T were previously determined for **3a** (0.4 μs) [12] in benzene and **4a** (3.0 μs) [3] in MeCN. For the triplet of **2a**, a similar lifetime of 3.0 μs was found in benzene [20].

The triplet lifetimes of the initiators **1a** and **1b** were estimated by means of energy transfer to naphthalene, monitoring the growing in of the acceptor triplet at $\lambda = 412$ nm [21] in MeCN upon irradiation at 355 nm. Naphthalene has been shown to quench the triplets of **1a** efficiently; [3] the same should hold true for the triplets of **1b**. Linear Stern-Volmer plots were obtained for both **1a** and **1b**, allowing the determination of the products of quenching rate constant (k_q) and triplet lifetime (τ_T) from the slopes.

The value of τ_T for **1a** was calculated to be $\tau_T = 0.58$ ns using $k_q = 7.4 \times 10^9 \text{ M}^{-1} \text{ s}^{-1}$ [3], in good agreement with the literature value (0.37 ns) [3]. Since the value of k_q was not available for **1b**, we used the triplet decay of the structurally similar, but photo-

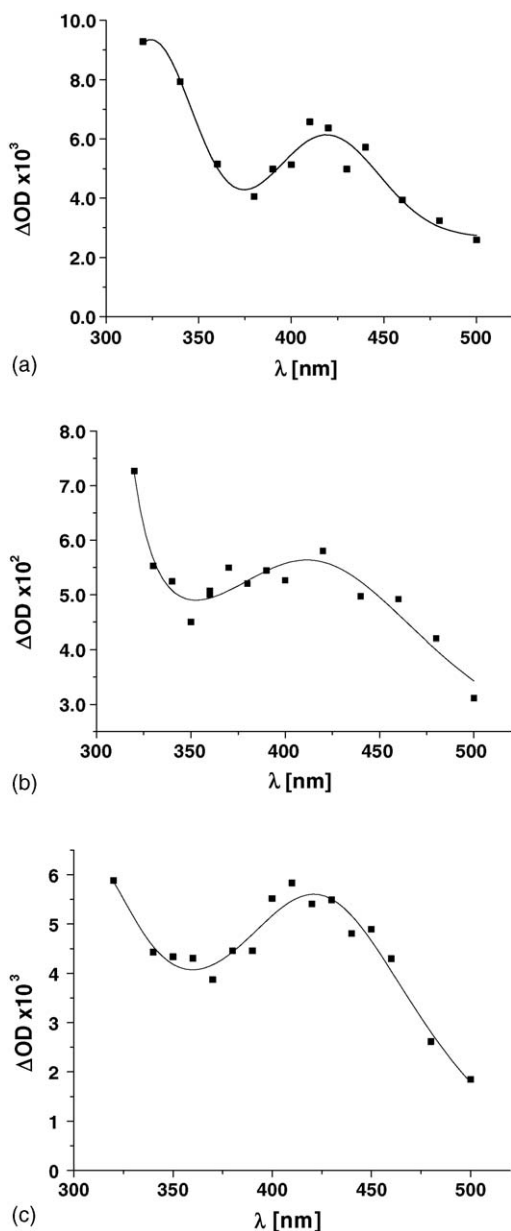


Fig. 2. Triplet–triplet absorption spectra of **2b** (panel a), **3b** (panel b) and **4b** (panel c) in MeCN ($\lambda_{\text{exc}} = 266$ nm).

stable derivative **4b** for its experimental estimation. Treatment of the decay rate of the triplet–triplet absorption of **4b** at 440 nm in presence of naphthalene according to pseudo-first-order kinetics yielded a quenching rate constant $k_q = 9.1 \times 10^9 \text{ M}^{-1} \text{ s}^{-1}$. Using this value gives a triplet lifetime $\tau_T = 1.0$ ns for **1b**, about twice longer than that of the reference compound **1a**.

The naphthalene energy transfer experiment further allowed an estimation of the quantum yield of triplet formation (Φ_T), whose magnitude is one of the limiting steps as regards the efficiency of photocuring. To this end, the extrapolated y-axis intercepts of the Stern-Volmer plots were used to calculate a limiting energy transfer efficiency based on an extinction coefficient for the triplet–triplet absorption of naphthalene, $\varepsilon_{412} = 14500 \text{ M}^{-1} \text{ cm}^{-1}$ in MeCN [21]. Using this method, a smaller value was obtained for **1b** ($\Phi_T = 0.10$) compared to **1a**

Table 1

Photophysical properties of photoinitiators and their derivatives in acetonitrile

Compound	$\lambda_{\text{max}}^{\text{T-T}}$ (nm) ^a	τ_T (ns) ^b	Φ_T^c
1a	320 ^d	0.58	0.25
1b	– ^e	1.00	0.10
2a	320	230	1.00
2b	410	3000	1.00
3a	335	370	0.80
3b	430	170	– ^e
4a	335	3000	– ^e
4b	420	1500	0.52

^a $\lambda_{\text{max}}^{\text{T-T}}$, triplet–triplet absorption maximum in acetonitrile.

^b τ_T , triplet lifetime in acetonitrile at 20 °C.

^c Φ_{ISC} , quantum yield of triplet formation.

^d From Ref. [3].

^e Not determined.

($\Phi_T = 0.25$), the latter being in good agreement with the literature value of 0.2–0.3 [22]. The ester **4b** exhibited a Φ_T of 0.52. For acetylpyridine **2b** Φ_T was determined to be 1.0 using triplet energy transfer to anthracene at $\lambda_{\text{exc}} = 266$ nm; the same value had been reported for Φ_T of **2a** [23]. All obtained values and literature data are summarized in Table 1.

3.2. Photochemistry of **1a** and **1b**

3.2.1. Steady-state photolysis

Steady-state photolysis (SSP) experiments (365 nm) of 1×10^{-4} M solutions of the initiators **1a** and **1b** suggested similar photochemistry (Fig. 3).

The kinetics in MeCN (365 nm) at equal light absorption for **1a** (1×10^{-2} M) and **1b** (5×10^{-3} M) were determined by HPLC (Fig. 4a). The data were fitted to second-order polynomials, from which initial rate constants (R_D) were calculated, yielding a twice higher value for **1a** ($R_D = 9.39 \times 10^{-6} \text{ M s}^{-1}$) compared to **1b** ($R_D = 5.32 \times 10^{-6} \text{ M s}^{-1}$).

Using radical trapping with TEMPO and product analysis, we had previously established the formation of nicotinic acid 2,2,6,6-tetramethyl-piperidin-1-yl ester (**5b**) upon steady-state photolysis of both **1b** and **3b**, demonstrating the intermediate production of a nicotinoyl radical [7].

Kinetic analysis was done by irradiation of 1×10^{-2} M solutions of **1a** and **1b** in MeCN at 365 nm in the presence of two equivalents of TEMPO (2×10^{-2} M).

Similar rates for degradation (R_D) and product formation (R_{PP}) were found for **5a** and **5b** (Fig. 4b). Surprisingly **1b** degraded twice faster in the presence of TEMPO than in its absence. This might indicate suppression of a recombination reaction between the nicotinoyl radical and the hydroxypropyl radical.

The quantum yields of decomposition, Φ_D and the quantum yields of photoproduct formation, Φ_{PP} were determined by actinometry (see Section 2.5). Values around 0.6 were obtained in all cases with the exception of the degradation of **1b** in the absence of TEMPO which gave $\Phi_D = 0.29$ (Table 3). The previously published values of the α -cleavage quantum yield, Φ_α of **1a** in non-hydrogen donating solvents scatter considerably. Ruhlmann et al. reported a value of 0.29 [24], estimated by LFP

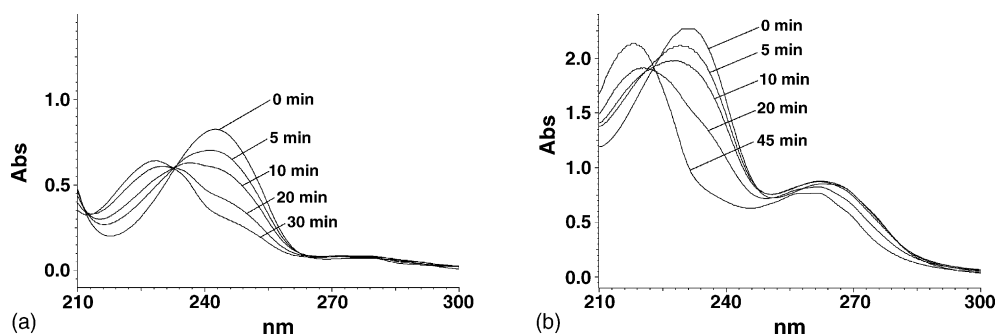


Fig. 3. Steady-state photolysis of **1a** (a) and **1b** (b) in 1×10^{-4} M solution in MeCN.

experiments, while Jockusch et al. obtained $\Phi_{\alpha} = 0.38$ by means of ground state bleaching of an oxygen-saturated solution [3]. More recently, Allonas et al. reported a Φ_{α} of 0.8 based on photoacoustic calorimetry and molecular modeling [25].

It is notable that all quantum yield values determined in steady-state photolysis experiments are higher than the quantum yield of triplet formation obtained by energy transfer to naphthalene by means of laser flash photolysis (Table 1). The reason for this discrepancy is not clear at present. Textbook knowledge states that α -cleavage is generally about 10^2 times slower from the singlet state than from the triplet state for usual ketones [26]; this seems to preclude this possibility. The occurrence of secondary degradation steps initiated by radical attack on the substrate is unlikely, especially in solutions containing TEMPO. The most plausible interpretation seems to be that α -cleavage is possible from higher $n-\pi^*$ triplet states which are too short-lived to transfer their energy to naphthalene; it might even be that all photochemistry occurs in this way while the lowest triplet state is not photoactive.

3.2.2. Radical spectra

The end-of-pulse transient spectra detected upon laser flash photolysis of **1a** and **1b** in MeCN upon excitation of diluted deaerated solutions (5×10^{-4} M to 2×10^{-3} M) at 266 nm showed maxima at 360 and 370 nm, respectively (Fig. 5). These transients cannot be ascribed to triplet states because of the short lifetime of the latter (see above). Benzoyl radicals with

an absorption maximum around 370 nm have previously been reported upon pulse radiolysis of benzoyl chloride [27]. The pivaloylketone **3b**, which is α -cleavable as well, showed a long lived transient with a maximum at 380 nm (Fig. 5); the *tert*-butyl radicals formed in this case have been characterized by absorption maxima at 220 and 307 nm [28]. The 360–370 nm bands obtained in our experiments are therefore plausibly assigned to benzoyl, resp. nicotinoyl radicals. Under the conditions of this experiment, both radicals decayed predominantly by second-order kinetics, although first-order or pseudo-first order components could not be excluded at higher substrate concentrations (Fig. 6).

The dependences of the transient absorption on pulse energy were found to be linear; the product of the extinction coefficient and the quantum yield of radical formation ($\epsilon\Phi$) were calculated from the slopes. Using the values of Φ_D from steady-state photolysis in the absence of TEMPO (Table 2), ϵ could be estimated for both radicals, leading to ϵ_{370} for the benzoyl radical of $\sim 200 \text{ M}^{-1} \text{ cm}^{-1}$ and $\epsilon_{370} \sim 300 \text{ M}^{-1} \text{ cm}^{-1}$ for the nicotinoyl radical. For the benzoyl radical, an ϵ_{370} of $\sim 150 \text{ M}^{-1} \text{ cm}^{-1}$ has been found by Fischer et al. [29] and is in good agreement with our results.

3.2.3. Radical kinetics

The reactivity of the radicals formed by photoinitiator α -cleavage is one of the keys to polymerization efficiency. In the following, we compare the reactivity of benzoyl radicals with

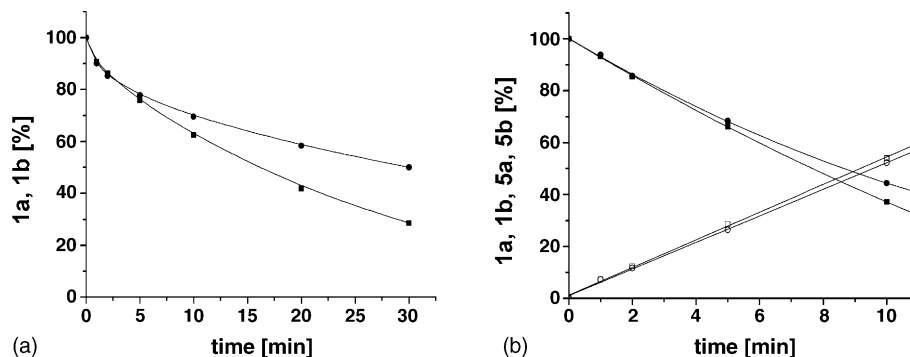


Fig. 4. (a) Time course of photoinduced degradation of **1a** (—■—, 1×10^{-2} M) and **1b** (—●—, 5×10^{-3} M) in MeCN ($\lambda_{\text{exc}} = 365$ nm). (b) Photodegradation of **1a** (—■—) and **1b** (—●—) and buildup of the photoproducts **5a** (—□—) and **5b** (—○—) upon irradiation (365 nm) of 1×10^{-2} M solutions in MeCN in the presence of 2×10^{-2} M TEMPO.

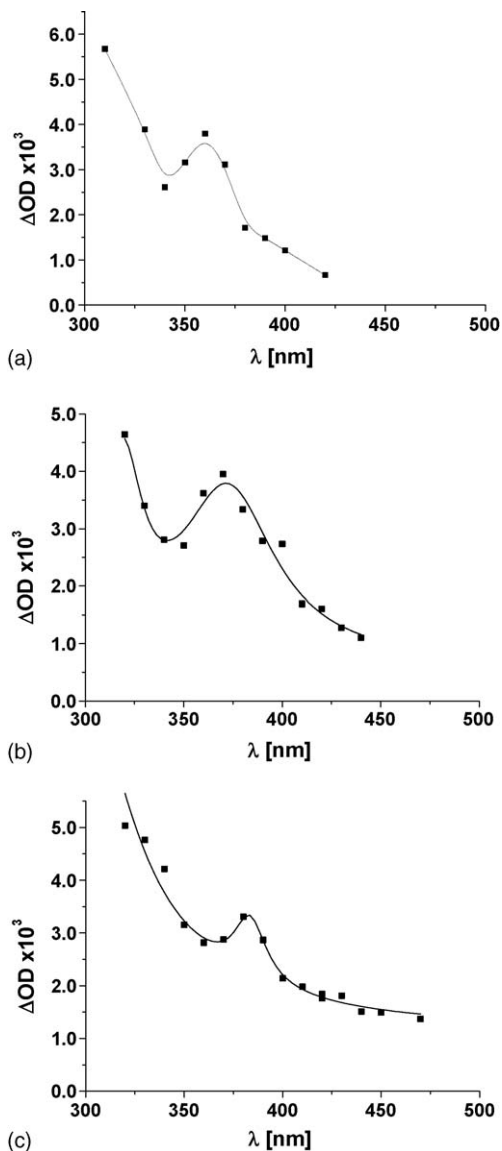


Fig. 5. Transient spectra of **1a** (panel a) and **1b** (panel b) at pulse end and **3b** (panel c) at 40 μ s obtained upon laser flash photolysis in MeCN at 266 nm.

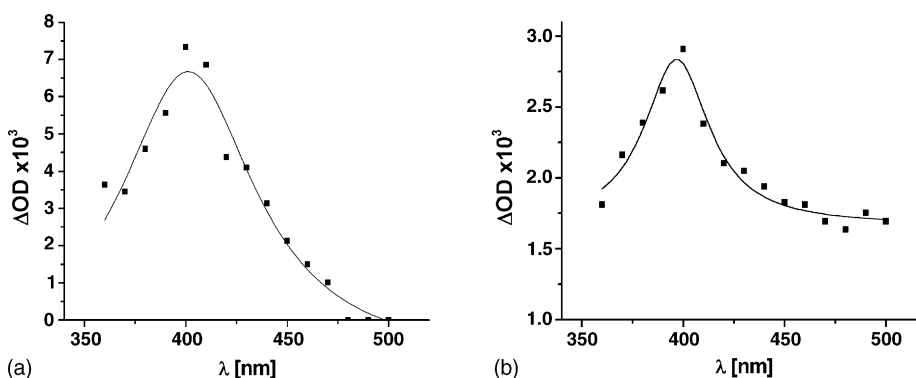


Fig. 6. Spectrum of the benzoylperoxyl radical (a) and nicotinoylperoxyl radical (b) obtained upon laser flash photolysis of **1a** and **1b** in O_2 -saturated MeCN.

that of nicotinoyl radicals towards molecular oxygen, TEMPO, and methyl methacrylate (MMA). The results are summarized in Table 3.

3.2.3.1. Reaction with molecular oxygen. Oxygen inhibition is known to be one of the major problems in light-induced free radical polymerization. In this respect, it was encouraging that photo-DSC experiments under air indicated a decreased oxygen sensitivity of the pyridine initiator **1b** compared to **1a** in terms of double bond conversion and rate of polymerization [7].

Three types of interaction can be made responsible for the oxygen effect on photoinduced radical polymerization: quenching of the photoinitiator triplet state, reaction with primary radicals, and reaction with radicals in the propagating chain. Due to the fast cleavage of the initiators **1a** and **1b** triplet quenching by oxygen can be excluded under ambient oxygen concentrations ($[O_2] < 2$ mM). On the other hand, it is well known that oxygen efficiently reacts with the radicals on the growing chain. A specific influence of the pyridine moiety on the propagating chain reaction could be excluded by photo-DSC experiments with additional pyridine or 3-acetylpyridine in the formulation [7]. Considering the primary radicals, both initiators formed the dimethylketyl radical which therefore could not be responsible for the different behavior under oxygen. It was therefore of interest to study the reactions of the benzoyl and nicotinoyl radicals with oxygen by means of laser flash photolysis.

The reaction of benzoyl radical with oxygen is known to be fast ($>10^9$ $M^{-1} s^{-1}$). The transient spectra at pulse end measured in oxygen-saturated acetonitrile (~ 6.7 mM) of **1a** should therefore derive from the benzoylperoxyl radical. A maximum at 400 nm was found (Fig. 6a) as described in the literature [30]. A similar absorption band was obtained from **1b** in the same conditions (Fig. 6b). The assignment of this transient to the nicotinoylperoxyl radical is further supported by the earlier observation that nicotinic acid is a product of the steady-state photolysis of **1b** under air [7]; bimolecular decomposition of these radicals gives nicotinoyloxy radicals which after hydrogen abstraction yield nicotinic acid.

The rate constants for reaction of benzoyl and nicotinoyl radicals with O_2 were determined by measurement of the build-up kinetics of the peroxyl radical at 400 nm as a function of O_2 concentration, varied by purging the solution with mixtures of

Table 2
Kinetic data and quantum yields of **1a** and **1b** from steady-state photolysis in MeCN at 365 nm

PI	$c_{PI} \times 10^3$ (mol l ⁻¹) ^a	$c_T \times 10^3$ (mol l ⁻¹) ^b	$R_D \times 10^6$ (mol l ⁻¹ s ⁻¹) ^c	Φ_D ^d	$R_{PP} \times 10^6$ (mol l ⁻¹ s ⁻¹) ^e	Φ_{PP} ^f
1a	9.50	–	9.39	0.60	–	–
1a /TEMPO	9.63	19.4	11.4	0.66	8.84	0.57
1b	9.86	–	4.71	0.29	–	–
1b /TEMPO	10.1	19.3	10.2	0.63	8.87	0.55

^a Concentration of the initiators.

^b Concentration of TEMPO.

^c Rate of decomposition.

^d Quantum yield of decomposition.

^e Rate of photoproduct formation.

^f Quantum yield of photoproduct formation.

Table 3
Rate constants k (M⁻¹ s⁻¹) of benzoyl and nicotinoyl radicals with various reactants

Reactant	Benzoyl radical	Nicotinoyl radical
Oxygen	4.4×10^9	2.6×10^9
TEMPO	9.6×10^6	1.8×10^8
MMA	8.3×10^5	7.6×10^5

oxygen/argon (Fig. 7). The O₂ concentration was determined by recording the decay kinetics of anthracene triplets in the same purging conditions, using the equilibrium concentration of oxygen in air-saturated acetonitrile (2.4×10^{-3} M) [29].

It is obvious that the benzoyl radical reacts almost twice faster with oxygen ($k = 4.4 \times 10^9$ M⁻¹ s⁻¹) than the nicotinoyl radical ($k = 2.6 \times 10^9$ M⁻¹ s⁻¹).

The smaller rate constant for reaction of the primary radical with O₂ is therefore a possible reason for the decreased oxygen sensitivity of the pyridine initiator **1b** compared to **1a**.

3.2.3.2. *Quenching experiments with TEMPO.* The rate constants for the reaction of the benzoyl and nicotinoyl radicals with TEMPO were determined by pseudo-first order treatment of the decays at 380 nm at various TEMPO concentrations (Fig. 8).

The results demonstrate that the rate constant for the reaction of the nicotinoyl radical with TEMPO ($k_{\text{TEMPO}} = 1.6 \times 10^8$ M⁻¹ s⁻¹) is about 17 times higher compared to the value for the benzoyl radical ($k_{\text{TEMPO}} = 9.6 \times 10^6$ M⁻¹ s⁻¹).

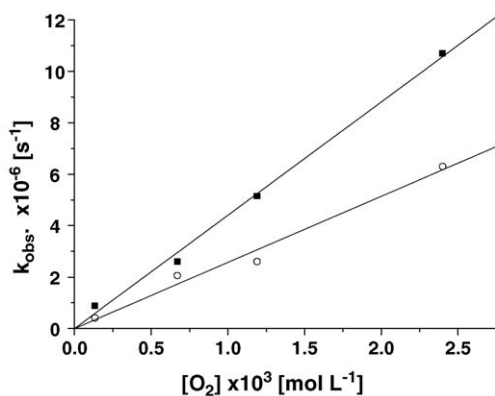


Fig. 7. Determination of the rate constants of radical reaction with O₂:benzoyl radicals (from **1a**) (—■—), nicotinoyl radicals (from **1b**) (—○—).

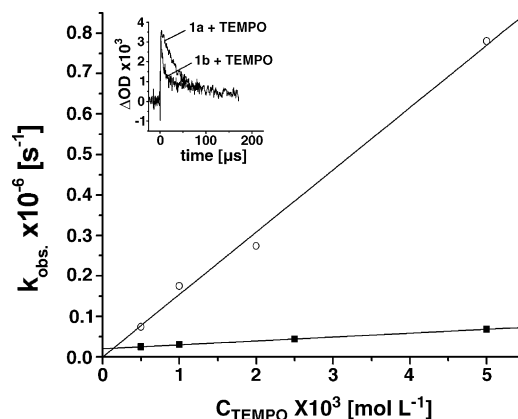


Fig. 8. Radical reaction with TEMPO:benzoyl radicals (from **1a**) (—■—), nicotinoyl radicals (from **1b**) (—○—). Inset: radical decay at 380 nm at [TEMPO] = 1×10^{-3} M.

3.2.3.3. *Quenching experiments with MMA.* In view of the differences in the reactions of the nicotinoyl radical with TEMPO and oxygen compared to the benzoyl radical, it was of interest to study the radical reaction with a polymerizable double bond. To this end, solutions of the photoinitiators in MeCN (10^{-2} M) were irradiated at 355 nm in the presence of methyl methacrylate; radical decay was monitored at 380 nm (Fig. 9).

Despite the large scatter of data points it is obvious that the reaction rate constants for both radicals with MMA are in the same order of magnitude, yielding values of $k_{\text{MMA}} = 8.3 \times 10^5$ M⁻¹ s⁻¹ for the benzoyl radical and $k_{\text{MMA}} = 7.6 \times 10^5$ M⁻¹ s⁻¹ for the nicotinoyl radical.

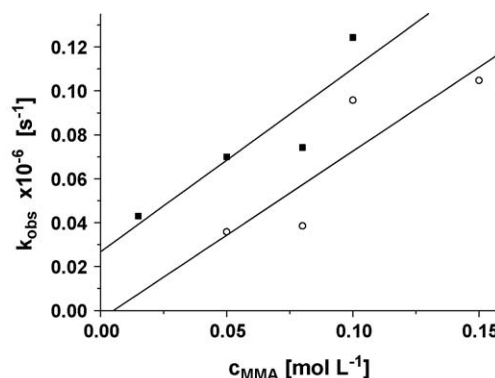


Fig. 9. Reaction of the radicals with MMA:benzoyl radicals (from **1a**) (—■—), nicotinoyl radicals (from **1b**) (—○—).

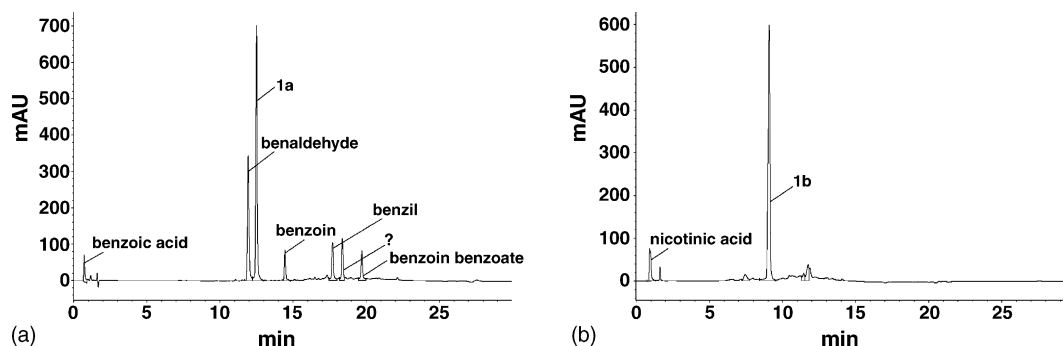


Fig. 10. HPLC analysis of the photolysis of (a) **1a** and (b) **1b** in MeCN after 30 min irradiation; n.i., not identified.

$10^5 \text{ M}^{-1} \text{ s}^{-1}$ for the nicotinoyl radical. On the other hand, the y-axis intercept values are different; while that of the nicotinoyl radical data is negligibly small, that for the benzoyl radical data is significant and comparable to that obtained with TEMPO (Fig. 8). This shows that in the absence of quenchers the decay of the benzoyl radical involves a component that limits its lifetime to about $50 \mu\text{s}$ at the specific radical concentration of this experiment, whereas the nicotinoyl radical appears to be much longer-lived. This result may be related to the impossibility to detect photolysis end-products, described in the next section.

3.2.4. Product studies

To identify the products of photochemical conversion, the photoinitiators **1a** and **1b** were irradiated in a Heraeus photoreactor for 5 h under oxygen-free conditions. High concentrations ($5 \times 10^{-2} \text{ M}$) in MeCN (400 ml) were used to obtain a sufficient amount of photoproducts for analysis.

As expected, steady-state photolysis of **1a** yielded benzaldehyde, benzil and benzoin after column chromatography as the known major photoproducts. Additionally, benzoic acid 2-oxo-1,2-diphenyl-ethyl ester was isolated as a reaction product of benzil with a benzoyl radical in $\sim 5\%$ yield [31]. HPLC analysis of the irradiated mixture shows that these compounds are the major photoproducts (Fig. 10a). One additional photoproduct was detected which could not be isolated by column chromatography. The reduction product of **1a** with the hydroxypropyl radical, 2-methyl-1-phenyl-1,2-propanediol as described by Allen et al. [32] was not formed in detectable amounts; this was checked by testing a reference standard prepared by reduction of **1a** with lithium aluminium hydride, which gave a peak after 10.44 min in the HPLC analysis.

In sharp contrast, steady-state photolysis of the initiator **1b** ($5 \times 10^{-2} \text{ M}$) in MeCN neither produced the expected recombination product of the nicotinoyl radical, 3,3'-pyridil, nor 3-pyridinealdehyde. Only small amounts of nicotinic acid (4%) could be isolated by column chromatography after 5 h irradiation, probably reflecting the presence of traces of oxygen. Most of the initiator **1b** was recovered. These results were confirmed by HPLC analysis (Fig. 10b). The possibility that 3,3'-pyridil might escape detection because of its own photodecomposition was disproved by testing the photostability of this compound in the same irradiation conditions, which proved to be high.

This unexpected failure to detect the expected photoproducts points to a fundamental difference in the reaction mechanism of photodegradation between **1a** and **1b**. At present, we can only speculate about the possible reasons. A major role seems to be played by the concentration of **1b**, since photolysis at low concentration did lead to an appreciable change of the UV spectrum (Fig. 3). A possible degradation bottleneck might reside in the reversible formation of radical-substrate adducts, which might impede nicotinoyl radical-radical coupling at high substrate concentrations. In addition, the balance of recombination versus radical-radical coupling might be shifted towards the former step in **1b** as compared to **1a**, as suggested by the smaller initial photodegradation quantum yield (Table 2). It must however be stressed that this specific behavior of **1b** is only valid in the absence of reaction partners, and therefore not significant for the understanding of the photopolymerization process.

4. Conclusions

In the present work, we have studied and compared the photophysical and photochemical behavior of two polymerization photoinitiators, 2-hydroxy-2-methyl-1-phenylpropan-1-one (Darocur 1173[®], **1a**) and its pyridine analogue 2-hydroxy-2-methyl-1-pyridin-3-yl-propan-1-one (**1b**), and some of their derivatives. Besides giving the first account of the photophysical and photochemical properties of the group of pyridine derivatives, the results obtained by means of nanosecond transient absorption spectroscopy and steady-state photolysis allowed a rationalization of an earlier study of polymerization photoinitiation using **1b** [7]. Both initiators are quite similar regarding most of the studied triplet state and radical reactivity data. The triplet yield, measured by energy transfer to naphthalene, is smaller for **1b** ($\Phi_T = 0.10$) than for **1a** ($\Phi_T = 0.25$), but both substances had high photodegradation quantum yields ($\Phi_D = 0.6$) in the presence of TEMPO. This discrepancy between triplet and photodegradation yields was unexpected and points to the possibility of the occurrence of α -cleavage in higher excited triplet states. The study of the reactivity of the radicals produced upon α -cleavage, benzoyl radical from **1a** and nicotinoyl radical from **1b**, demonstrated that both species have comparable reactivity towards polymerizable double bonds, but that the nicotinoyl radicals reacts 17 times faster with TEMPO than the benzoyl radical. Most importantly, we were able to

show that the previously observed reduced oxygen sensitivity of **1b** compared to **1a** [7] can be traced to a smaller reactivity towards O₂ of the nicotinoyl radical compared to the benzoyl radical.

References

- [1] J.P. Fouassier, Photoinitiation, Photopolymerization and Photocuring, Hanser Publishers, Munich, 1995.
- [2] H.F. Gruber, Prog. Polym. Sci. 17 (1992) 953–1044.
- [3] S. Jockusch, M.S. Landis, B. Freiermuth, N.J. Turro, Macromolecules 34 (2001) 1619–1626.
- [4] R. Liska, Heterocycles 55 (8) (2001) 1475–1486.
- [5] R. Liska, S. Knaus, J. Wendrinsky, Nucl. Instrum. Meth. Phys. Res. Sect. B 151 (1999) 290–292.
- [6] T.S. Cantrell, J. Org. Chem. 39 (15) (1974) 2242–2246.
- [7] R. Liska, D. Herzog, J. Polym. Sci. Part A 42 (2004) 752–764.
- [8] S.K. Sarkar, S.K. Ghoshal, G.S. Kastha, Proc. Indian Acad. Sci. 92 (1983) 47–58.
- [9] P. Traynard, J.P. Blanchio, Mol. Photochem. 4 (2) (1972) 223–234.
- [10] P.J. Wagner, H.N. Schott, J. Am. Chem. Soc. 91 (1969) 5383–5384.
- [11] P.J. Wagner, G. Capen, Mol. Photochem. 1 (2) (1969) 173–188.
- [12] I. Naito, R. Kuhlmann, W. Schnabel, Polymer 20 (1979) 165–170.
- [13] C.S. Barnes, E.J. Halbert, R.J. Goldsack, Aust. J. Chem. 26 (1973) 2027–2034.
- [14] C. Bolm, M. Ewald, M. Felder, G. Schlingloff, Chem. Ber. 125 (1992) 1169–1190.
- [15] A. Fuerstner, D.N. Jumbam, Tetrahedron 48 (1992) 5991–6010.
- [16] W.Y. Suprun, J. Prakt. Chem. Chem. Ztg. 340 (3) (1998) 247–255.
- [17] P. Baranyai, S. Gangl, G. Grabner, M. Knapp, G. Köhler, T. Vidóczy, Langmuir 15 (22) (1999) 7577–7584.
- [18] B. Seidl, R. Liska, Proceedings of the RadTech Europe 2003, vol. 2, 2003, pp. 999–1007.
- [19] K. Willett, R. Hites, J. Chem. Educ. 77 (2000) 900–902.
- [20] H. Lutz, L. Lindqvist, J. Chem. Soc. D Chem. Commun. (1971) 493–494.
- [21] G. Grabner, K. Rechthaler, B. Mayer, G. Köhler, K.J. Rotkiewicz, J. Phys. Chem. A 104 (7) (2000) 1365–1376.
- [22] J. Eichler, C.P. Herz, I. Naito, W. Schnabel, J. Photochem. 12 (1980) 225–234.
- [23] S.K. Chattopadhyay, C.V. Kumar, J. Photochem. 30 (1985) 81–91.
- [24] D. Ruhlmann, J.P. Fouassier, W. Schnabel, Eur. Polym. J. 28 (3) (1992) 287–292.
- [25] X. Allonas, J. Lalevée, J.P. Fouassier, J. Photochem. Photobiol. A 159 (2003) 127–133.
- [26] N.J. Turro, Modern Molecular Photochemistry, University Science Books, Sausalito, 1991, p. 530.
- [27] W. Knolle, U. Müller, R. Mehnert, Phys. Chem. Chem. Phys. 2 (2000) 1425–1430.
- [28] C. Huggenberger, H. Fischer, Helv. Chim. Acta 64 (1981) 338–353.
- [29] H. Fischer, R. Baer, R. Hany, I. Verhoolen, M. Walbiner, J. Chem. Soc. Perkin Trans. 2 (1990) 787–798.
- [30] T. Hancock-Chen, J.C. Scaiano, Photochem. Photobiol. 67 (1998) 174–178.
- [31] F.D. Lewis, R.T. Lauterbach, H.G. Heine, W. Hartmann, H. Rudolph, J. Am. Chem. Soc. 97 (6) (1975) 1519–1525.
- [32] N.S. Allen, M.C. Marin, M. Edge, D.W. Davies, J. Garrett, F. Jones, S. Navaratnam, B.J. Parsons, J. Photochem. Photobiol. A 126 (1999) 135–149.